On the Nature of Calcium Ion Binding between Phosphatidylserine Lamellae†

G. W. Feigenson

Section of Biochemistry, Molecular and Cell Biology, Cornell University, Ithaca, New York 14853

Received April 25, 1986; Revised Manuscript Received June 5, 1986

ABSTRACT: Ca^{2+} binding between phosphatidylserine (PS) lamellae gives rise to a phase with the composition $Ca(PS)_2$. When aqueous Ca^{2+}, hydrated PS, and $Ca(PS)_2$ coexist at equilibrium, the aqueous Ca^{2+} concentration is invariant. At Ca^{2+} concentrations below this critical value, no binding of Ca^{2+} to PS is detected. Above this value, Ca^{2+} binds to PS to form $Ca(PS)_2$. The invariant Ca^{2+} concentration is 0.14 μM for palmitoyloleoylphosphatidylserine (POPS) and 3.0 μM for dioleoylphosphatidylserine (DOPS). For the mixed acyl chain PS derived from bovine brain (BBPS) this Ca^{2+} concentration ranges from 0.25 to 0.7 μM. The observed phase behavior is described by the phase rule for the three-component system of water, Ca^{2+}, and PS, with temperature and pressure constant. In order for Ca^{2+} to bind between PS lamellae to form the $Ca(PS)_2$ phase, the aqueous Ca^{2+} concentration must be supersaturated. The equilibrium Ca^{2+} concentration is determined by dissolving $Ca(PS)_2$ by use of Ca^{2+} chelators.

An increase in intracellular Ca^{2+} concentration might influence the behavior of membrane lipids. Previous studies of the interaction of Ca^{2+} with phospholipids in *model* membrane systems have generally found that Ca^{2+} concentrations in the millimolar range are required to produce effects such as vesicle fusion or significant Ca^{2+} binding (Hendrickson & Fullington, 1965; Lansman & Haynes, 1975; Nir et al., 1978; Portis et al., 1979; Morris et al., 1979; McLaughlin et al., 1981; Eckerdt & Papahadjopoulos, 1981; Tilcock & Cullis, 1981; Silvius & Gagné, 1984). These concentrations are much greater than the maximum intracellular Ca^{2+} concentrations that have been associated with fusion [Llinás et al., 1976; see Campbell (1983) for a review]. However, Ca^{2+} binding at much lower concentrations is found for phosphatidylserine (PS)[1] lamellae that are in close proximity because of protein-induced aggregation (Hong et al., 1982) or initial multilamellar sample preparation (Ohnishi & Tokutomi, 1981). Papahadjopoulos and coworkers [see for example Portis et al. (1979)] have emphasized that the Ca^{2+} interaction at the aqueous PS surface is essentially different from the Ca^{2+} interaction between lamellae, bridging head groups. The implication of this difference is the necessity to measure and to characterize Ca^{2+} binding between PS lamellae.

Our approach to this problem is based on three principles: (i) It is easier to analyze binding to only one kind of site rather than two. Accordingly, lipid preparations are multilamellar, with unilamellar liposomes avoided in order to decrease the number of binding sites at the aqueous PS surface. (ii) Lipid bilayers are relatively impermeable to ions. Therefore, suitable means must be found to expose all binding sites to Ca^{2+}. (iii) The binding of Ca^{2+} to PS might be a cooperative phenomenon that yields a separate phase. Thus, supersaturation must be recognized and not confused with equilibrium. The supersaturation problem was recognized and solved by earlier workers in measuring solubility products [for a good example see Melcher (1910)]. Their procedure, also followed here, was first to prepare the compound by exceeding saturation and then to measure the amount that *dissolves* under the conditions of interest.

† This work was supported by grants from the National Institutes of Health, U.S. Public Health Service (HL-18255), and the National Science Foundation (DMB-85-10189).

Experimental Procedures

Materials

Dioleoylphosphatidylserine (DOPS), palmitoyloleoylphosphatidylserine (POPS), and bovine brain phosphatidylserine (BBPS), from Avanti Polar Lipids Inc. (Birmingham, AL), showed no impurities when 50 μg was chromatographed on Adsorbosil-5-P TLC plates using chloroform/methanol/concentrated NH_3, 25/10/2 by volume. Water was freshly purified through a Milli-Q system (Millipore Corp., Bedford, MA). Chelex-100 ion-exchange resin from Bio Rad (Rockville Center, NY) was cycled batchwise twice through 1 N HCl/1 N KOH. EGTA and Pipes buffer was puriss grade, arsenazo III p.a. grade, from A. G. Fluka (Hauppauge, NY). $CaCO_3$ and HCl were ultrex grade, and the phosphate standard was an analytical concentrate, from J. T. Baker (Bricktown, NJ). The calcium chelator/indicator BAPTA and BrBAPTA were from Molecular Probes (Junction City, OR). $^{45}CaCl_2$ and ACS scintillation fluid were from Amersham (Arlington Heights, IL). Ionomycin was from Calbiochem (San Diego, CA), X-537A (lasalocid, Na^+ salt) was from Aldrich (Milwaukee, WI), and A23187 was a gift from Eli Lilly and Co. (Indianapolis, IN). Other chemicals were reagent grade.

Methods

Preparation and Calibration of Solutions. All aqueous solutions contain 100 mM Pipes buffer and 100 mM KCl at pH 7.00. The buffer was stored in a polypropylene bottle over a bed of Chelex at 4 °C. Prior to use, the buffer was warmed to room temperature and then filtered through HCl-rinsed

[1] Abbreviations: PS, 1,2-diacyl-*sn*-glycero-3-phosphoserine with specified or unspecified cations bound to neutralize charge; DOPS, 1,2-dioleoyl-*sn*-glycero-3-phosphoserine; POPS, 1-palmitoyl-2-oleoyl-*sn*-glycero-3-phosphoserine; BBPS, 1,2-diacyl-*sn*-glycero-3-phosphoserine derived from bovine brain; Pipes, piperazine-*N*,*N*′-bis(2-ethanesulfonic acid); EDTA, ethylenediaminetetraacetic acid; EGTA, ethylene glycol bis(2-aminoethyl ether)-*N*,*N*,*N*′,*N*′-tetraacetic acid; BAPTA, 1,2-bis[bis(carboxymethyl)amino]ethane; BrBAPTA, 1,2-bis[[bis(carboxymethyl)amino](5-bromophenoxy)]ethane; M^{n+}, multivalent metal cation; K_D, dissociation constant; A_0, absorbance in the absence of M^{n+}; A_1, absorbance in excess M^{n+}; A_0', A_0 divided by the absorbance at the isosbestic point; A_1', A_1 divided by the absorbance at the isosbestic point; θ, fraction of total binding sites occupied by ligand; a_n, thermodynamic activity of n; ICP, inductively coupled plasma.

0006-2960/86/0425-5819$01.50/0

sintered glass to remove Chelex bead fragments.

A primary standard Ca^{2+} solution was prepared from $CaCO_3$ dried to constant weight. Approximately 1 g of $CaCO_3$ was dissolved in excess 6 N HCl, Pipes and KCl were added, the pH was adjusted to 7.00, and the volume was adjusted to 100.0 mL in a volumetric flask. Solutions of the Ca^{2+} chelators EGTA, BAPTA, and BrBAPTA were made to nominal concentration of 10–100 mM in Pipes–KCl buffer and pH then adjusted to 7.00. Actual concentrations were determined by titration with the Ca^{2+} standard using a Ca^{2+}-sensitive electrode (Radiometer) together with the pH meter (Fisher Accumet Model 810) operating in the millivolt mode. Triplicate determination of chelator concentrations showed standard deviation of 0.5%.

The concentrations of solutions of PS in chloroform were determined spectrophotometrically after lipid digestion in H_2SO_4 and H_2O_2, as previously described [Kingsley and Feigenson (1979) modified from Chen et al. (1956)].

Assay for Multivalent Cation Contamination. Following the general procedure used by Gratzer and Beaven (1977) to measure aqueous Ca^{2+} concentration, an arsenazo III assay was used to estimate multivalent cation *contamination*. The assay is sensitive to many different multivalent cations (Budesinsky, 1969). Arsenazo III, ~2 mM, stored over Chelex is added to the sample to give approximately 50–100 μM dye. Sample absorbance at 654 nm (A_{654}^{s}) is divided by absorbance measured in excess EDTA (A_{654}°) and the plot of $A_{654}^{s}/A_{654}^{\circ}$ vs. [EDTA] is compared with a standard plot. This assay is useful in the range ~2–50 μM Ca^{2+}, which can be extended by increasing or decreasing arsenazo III concentration.

With this assay, buffer–salt solutions in the 100–200 mM concentration range, prepared without special precautions, were found to contain 20–40 μM multivalent cation (M^{n+}) contamination. Storing these buffers over Chelex 100 reduced contamination below detection. Borosilicate culture tubes, 10 × 75 mm, released 4–8 μM M^{n+} to 200 μL of Pipes–KCl buffer over a 4-h period. Subjecting freshly prepared buffer to freezing and thawing caused M^{n+} release with each freeze/thaw cycle, with 8–12 μM M^{n+} found after 15 cycles. The amount of M^{n+} released by simple incubation or by freeze/thaw was found to be characteristic for each tube. Incubating with 10% HCl for 1 h followed by rinsing and drying reduced the M^{n+} released in 6 h into 200 μL of buffer from ~10 to 1–2 μM. By comparison, incubating tubes with EDTA, 0.5 M, pH 10, hardly reduced the release of M^{n+} under the same conditions. The HCl rinse was therefore used for all glassware used in Ca^{2+}-binding measurements.

Measurement of $[Ca^{2+}]$ *in the Micromolar Range.* Ca^{2+} chelators are used to define free aqueous Ca^{2+} concentrations and, in the case of indicator dyes, to measure $[Ca^{2+}]$ [see for example Campbell (1983)]. We use a value of the dissociation constant K_D for Ca–EGTA of 5.4×10^{-7} M as the basis value for all Ca^{2+} determinations. This value for the Ca–EGTA dissociation constant is derived from the measurement of $K_D = 4.9 \times 10^{-7}$ M reported by Grynkiewicz et al. (1985) for Ca–EGTA binding at 18 °C, pH 7.02, in 225 mM KCl and 25 mM NaCl, by making a correction to pH 7.00 as described by these investigators. These conditions are close in temperature and ionic strength to the conditions in the studies discussed herein. The K_D value for Ca–BrBAPTA under our conditions was determined, following Tsien (1980), by finding the x-axis intercept of the plot of log $[(A - A_0)/A_1 - A)]$ vs. log $[Ca^{2+}]$. A_0 is the absorbance of the Ca^{2+}-free BrBAPTA, A_1 is the absorbance of the Ca^{2+}–BrBAPTA complex, and A is the measured absorbance of the BrBAPTA at a given $[Ca^{2+}]$, all at 262 nm. $[Ca^{2+}]$ was established by adding measured quantities of Ca^{2+} and EGTA, with [EGTA] 100-fold greater than [BrBAPTA]. This procedure gives the K_D for Ca–BrBAPTA as 3.0 μM. A similar procedure for BAPTA under these conditions gives K_D as 0.27 μM. Once the K_D is established, the concentration of free (uncomplexed) Ca^{2+} is found from

$$[Ca^{2+}] = K_D \frac{[\text{Ca–chelator}]}{[\text{free chelator}]} = K_D \frac{(A' - A_0')}{(A_1' - A')} \quad (1)$$

where the prime indicates dividing the measured absorbance at a peak in the difference spectrum by the measured absorbance at the isosbestic point. We find for BrBAPTA, $A_0' = 1.38$ and $A_1' = 0.30$ with absorbance measured at 262 nm and the isosbestic point at 247.7 nm. For BAPTA, $A_0' = 1.44$ and $A_1' = 0.17$, with absorbance measured at 253 nm and the isosbestic point at 236.5 nm.

The $[Ca^{2+}]$ can also be determined from the value of K_D[Ca–chelator]/[free chelator] with [Ca–chelator] determined by liquid scintillation counting of β emission from ^{45}Ca and [free chelator] calculated from its initial concentration. This radioactivity procedure was always used in experiments involving EGTA without indicator dye present and also in experiments involving concentrations of BrBAPTA or BAPTA that exceed the absorbance limit of 4 for the Cary 219 spectrophotometer. With use of 5-mM path length cells, the maximum dye concentration used was 0.4 mM.

In all measurements of Ca^{2+} binding to PS, samples of 50–250 μL were centrifuged in 250-μL polyethylene centrifuge tubes, which were supported in 2 M sorbitol and centrifuged at 13 000 rpm for 1 h in an SW-27 swinging-bucket rotor at 21 °C. For samples of less than 200 μL, the centrifuge tubes were cut down in size in order to eliminate tube deformation during centrifugation. These centrifugation conditions pellet 99–100% of uncomplexed PS multilayers and 99.9–100% of $Ca(PS)_2$, as determined by phosphate analysis of the supernatant.

Protocols That Provide Ca^{2+} *Access between Lamellae.* In all of the procedures described below, except for the "Millipore filter method", chloroform solutions of PS were measured with a Hamilton gas-tight syringe into the bottom of an acid-washed 10 × 75 mm borosilicate culture tube. In some experiments the Ca^{2+} ionophores X-537A, A23187, or ionomycin were mixed with the PS in chloroform at a mole ratio of 1/500. Samples were dried under a stream of N_2 gas and then under mechanical pump vacuum, in the dark, overnight. Argon was used to relieve the vacuum. In one category of protocols, Pipes–KCl buffer was added to the dry film of PS, the tube sealed under argon, and the sample slowly rotated for 1–2 h at 21 °C in order to hydrate the lipid prior to Ca^{2+} addition. The appropriate amount of Ca^{2+} in Pipes–KCl buffer was then added. In the other category of protocols in which dry lipid is exposed to Ca^{2+}, Pipes–KCl buffer containing the appropriate amount of Ca^{2+} was added directly to the dry film of PS and the tube then sealed under argon. One of the protocols a–c was then followed:

(a) Samples were incubated at −10 °C for 1–4 min in a constant-temperature bath of KCl/ice (1/4 by weight). The supercooled but not frozen aqueous medium was nucleated to freeze by touching the glass tube just above the meniscus with a pipe cleaner dipped in liquid N_2. Samples were immediately returned to the −10 °C bath for 2–4 min in order to dissipate the latent heat of freezing. Samples were then removed to a water bath and thawed at room temperature. No significant difference in Ca^{2+} binding was observed when the samples were

thawed at 0–4 °C for 30 min or at 40 °C for 2 min. The cycle of freezing and thawing was repeated 15 times. As an index of the completeness of binding, we find that the binding of ^{45}Ca was unchanged after ~10 cycles.

(b) Samples were frozen in liquid N_2 for 15–20 s, removed to warm in the air for 3–15 min, and then placed in a room temperature water bath to complete the thawing. The cycle of freezing and thawing was repeated 15 times.

(c) Samples were slowly rotated (12 rpm) in the dark for 12–24 h.

After completion of the freezing/thawing cycles, or else at the end of the slow rotation period, tubes were opened, chelator in Pipes–KCl buffer added, and tubes resealed under argon. The 15 cycles of freezing/thawing, or else the 12–24 h of slow rotation, were repeated.

(d) Following the procedure described by Ohnishi and Ito (1974) with modifications as described, 5-μm Millipore cellulose filters were washed 2 to 3 times in benzene and air-dried. A piece of the filter approximately 5 × 10 mm was centrifuged to the bottom of each 10 × 75 mm acid-washed glass culture tube. A chloroform or else benzene solution of PS was added directly on to the filter. Benzene was then added to just saturate the filter. After a few minutes of incubation, the sample was dried in N_2 followed by overnight mechanical pumping. Each filter containing PS was then hydrated for 1–2 h in 200–400 μL of Pipes–KCl buffer under argon, in the dark. Ca^{2+} in Pipes–KCl buffer was then added, and the tubes were sealed under argon and then slowly rotated in the dark for 12–24 h. At the end of this period the chelator was added; the tubes were sealed under argon and again rotated slowly in the dark for 12–24 h. The temperature was 21 °C throughout this procedure.

Chemical Analysis of Ca(PS)$_2$. Samples of $Ca(PS)_2$ were prepared by adding excess Ca^{2+} to DOPS in Pipes–KCl buffer. After 15 cycles of liquid-N_2 freeze/room-temperature thaw, the precipitate was washed five times with 1-mL portions of water to remove aqueous Ca^{2+}. Samples of 1–2 mg were ashed in $HClO_4/HNO_3$ and analyzed for Ca and P in two separate determinations using a Jarrell-Ash Model 975 Plasma Atomcomp Inductively Coupled Plasma (ICP) spectrometer. Authentic samples of $CaHPO_4$, analyzed in this way, had stoichiometry of $Ca_{1.00}P_{1.00}$, ±3%.

Results

The nature of Ca^{2+} binding between PS lamellae was studied by equilibrating Ca^{2+} with DOPS using the protocols described above. The stoichiometry of Ca^{2+} binding to DOPS is found to be $Ca(PS)_2$, based upon the quantity of DOPS used and the unchanging quantity of Ca^{2+} bound at high $[Ca^{2+}]$. In order to verify this stoichiometry, $Ca(PS)_2$ was prepared at $[Ca^{2+}]$ = 1, 10, and 100 mM and analyzed by ICP spectrometry. The stoichiometries found using these values of $[Ca^{2+}]$ are $Ca_1P_{1.97}$, $Ca_1P_{2.04}$, and $Ca_1P_{2.02}$, respectively.

Data from many experiments are shown in Figure 1. These data are plotted as the fraction θ of occupied Ca^{2+} sites [assuming θ = 1 when all PS is in the form $Ca(PS)_2$] vs. the concentration of aqueous free Ca^{2+}. With initial [DOPS] of 0.20, 2.0, or 20.0 mM, the data shown in Figure 1 cover a range of final [DOPS] from 0.04 to 20 mM and a range of final $[Ca(PS)_2]$ from 0.002 to 10 mM. Data were obtained under conditions ranging from adding a small amount of Ca^{2+} and then dissolving 5–10% of the $Ca(PS)_2$ to reach a given value of θ to adding a much larger amount of Ca^{2+} and then dissolving up to 95% of the $Ca(PS)_2$ to reach a similar value of θ. The standard deviation in a value of θ is ~2% for θ near 0 and ~10% for θ near unity (because of the increased error

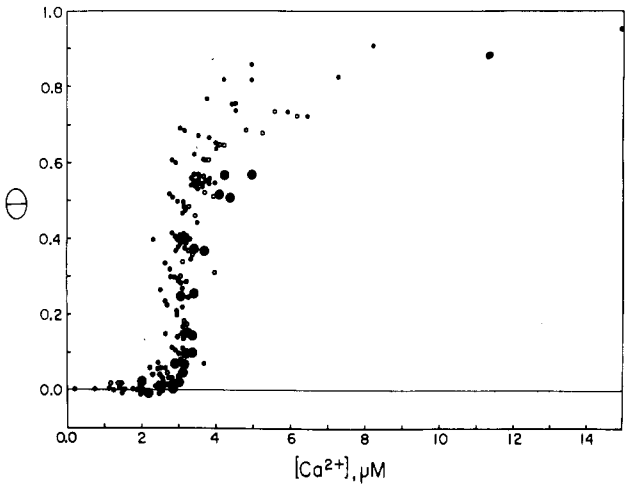

FIGURE 1: Ca^{2+} binding to multilamellar DOPS. The fraction θ of total DOPS present as $Ca(PS)_2$ is plotted against the measured free Ca^{2+} concentration $[Ca^{2+}]$: (●) total [PS] 20 mM; (•) total [PS] 2 mM; (○) total [PS] 0.2 mM. $[Ca^{2+}]$ was buffered with either EGTA or BrBAPTA. $[Ca^{2+}]$ was determined either by counting ^{45}Ca radioactivity or else by measuring BrBAPTA absorbance. The data were obtained by all of the different protocols described in the text to equilibrate Ca^{2+} across the PS lamellae.

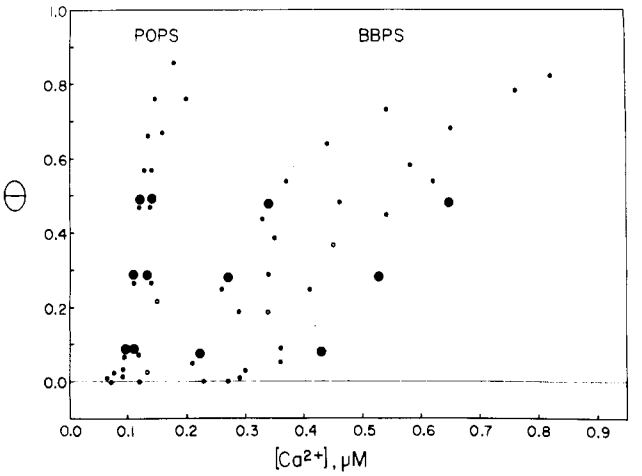

FIGURE 2: Ca^{2+} binding to multilamellar POPS and BBPS. The fraction θ of total POPS or BBPS present as $Ca(PS)_2$ is plotted against the measured free Ca^{2+} concentration $[Ca^{2+}]$: (●) total [PS] 20 mM; (•) total [PS] 2 mM; (○) total [PS] 0.2 mM. $[Ca^{2+}]$ was buffered with either BAPTA or BrBAPTA. $[Ca^{2+}]$ was determined by measuring chelator absorbance. The protocols used to equilibrate Ca^{2+} across the PS lamellae included incubating dry lipid with Ca^{2+} buffer for 12–24 h, 15× (liquid-N_2 freeze/thaw) of hydrated lipid, and 15× (−10 °C freeze/thaw) of hydrated lipid.

in subtraction as the amount of bound Ca^{2+} approaches the amount of possible binding sites). The standard deviation in a value of $[Ca^{2+}]$ is ~10% for concentrations near the K_D of Ca^{2+}–BrBAPTA of 3.0 μM but is larger for concentrations much less or much greater than 3 μM.

Figure 1 shows no detectable binding of Ca^{2+} to DOPS for $[Ca^{2+}] \lesssim 2.5$ μM. At $[Ca^{2+}] \sim 3.0$ μM, the binding plot becomes almost vertical, θ increasing as Ca^{2+} binds to DOPS at an almost constant $[Ca^{2+}]$. The plot changes shape at $\theta \sim 0.7$, with $[Ca^{2+}]$ now increasing as θ approaches unity.

Ca^{2+}-binding measurements are shown in Figure 2 for two other types of PS. For POPS, the low values of $[Ca^{2+}]$ that describe the binding could not be measured accurately using BrBAPTA. For this reason all of the measurements shown for POPS, and most for BBPS, use BAPTA as the chelator and spectrophotometric indicator. Fewer measurements were made with these lipids than with DOPS, but still the data cover

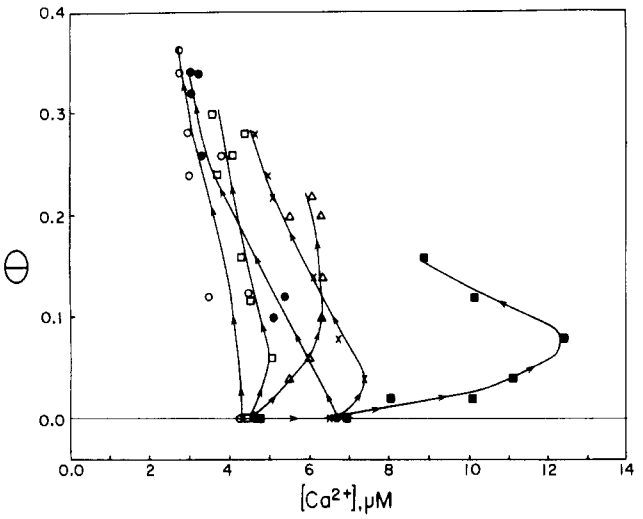

FIGURE 3: Supersaturation of Ca^{2+} binding to multilamellar DOPS. The fraction θ of total DOPS present as $Ca(PS)_2$ is plotted against the measured free Ca^{2+} concentration. Ca^{2+}–BrBATPA buffers with initial free $[Ca^{2+}]$ = 3–40 μM and [BrBAPTA] = 0.40 mM were added to 1 mM DOPS samples using the following protocols: (○) Ca^{2+} added to dry lipid, 15× (liquid-N_2 freeze/thaw); (●) Ca^{2+} added to hydrated lipid, 15× (liquid-N_2 freeze/thaw); (□) Ca^{2+} added to dry lipid, 15× (−10 °C freeze/thaw); (■) Ca^{2+} added to hydrated lipid, 15× (−10 °C freeze/thaw); (△) Ca^{2+} added to dry lipid, incubated 21 °C 12 h; (×) Ca^{2+} added to lipid hydrated on Millipore filter, incubated 12 h. Arrowheads indicate increasing initial $[Ca^{2+}]$.

initial PS concentrations of 0.20, 2.0, and 20.0 mM, and varied binding protocols were used (freeze/thaw at −10 °C; freeze/thaw at liquid-N_2 temperature; slow rotation; Millipore filter). With POPS, no Ca^{2+} binds up to ~0.12 μM. At ~0.14 μM Ca^{2+} binds and θ increases to ~0.7 almost without a change in $[Ca^{2+}]$. The shape of the plot for BBPS is somewhat different, with $[Ca^{2+}]$ increasing gradually from ~0.25 to ~0.7 μM as θ increases to ~0.7. However, for BBPS there is also no Ca^{2+} binding until a definite $[Ca^{2+}]$ is reached, in this case ~0.24 μM.

The binding measurements shown in Figures 1 and 2 result from experiments designed to avoid supersaturation effects by first exceeding saturation, then dissolving $Ca(PS)_2$, and finally measuring the equilibrium value of $[Ca^{2+}]$. In contrast, Figure 3 shows the supersaturation observed when Ca^{2+} binding to DOPS is measured as $[Ca^{2+}]$ is *gradually* increased. Six different protocols, described in the legend, were used to examine this behavior. These protocols differ from those described above only in the absence of a step to dissolve $Ca(PS)_2$ prior to measuring $[Ca^{2+}]$. Supersaturation is observed in every case, although the extent of supersaturation before Ca^{2+} binding begins depends upon the method, as does the final $[Ca^{2+}]$ at the end of the experiment. For several of the protocols, the final $[Ca^{2+}]$ approaches the equilibrium value of ~3.0 μM.

Discussion

General Nature of the Binding. The stoichiometry of Ca^{2+} binding to PS lamellae is established to be $Ca(PS)_2$ in the experiments described herein, on the basis of measurements of Ca^{2+} binding at high $[Ca^{2+}]$ and chemical analysis of the binding product. At equilibrium

$$Ca(PS)_2 + \text{water} \rightleftharpoons Ca^{2+}(aq) + 2PS(aq) \qquad (2)$$

The dissociation constant, expressed using thermodynamic activities, is

$$K_D = (a_{Ca^{2+}})(a_{PS_2})/a_{Ca(PS)_2} \qquad (3)$$

The data in Figure 1 show that over a 500-fold range of the final value of [DOPS], a 5000-fold range of final $[Ca(PS)_2]$, and a 3000-fold range of $[PS]/[Ca(PS)_2]$ (i.e., θ = 0.0002–0.7), the value of $[Ca^{2+}]$ is *almost constant*. The relationship between thermodynamic activity and measured concentration can be written for Ca^{2+} as $a_{Ca^{2+}} = \gamma[Ca^{2+}]$. γ, the activity coefficient, is not well-known for our conditions, but more important, it is a constant for our conditions of micromolar levels of $[Ca^{2+}]$ in the presence of ~200 mM salts. The almost constant value of $[Ca^{2+}]$ as long as both DOPS and $Ca(PS)_2$ coexist, given the constant value of K_D, therefore implies that neither a_{PS_2} nor $a_{Ca(PS)_2}$ changes with the "concentration" of these substances. Such constancy of thermodynamic activity as the amount of a substance varies is the hallmark of a pure phase. Thus, in our study, PS and $Ca(PS)_2$ each behave as a pure phase when both are coexisting with an aqueous Ca^{2+} phase. This conclusion enables us to apply the phase rule (Findlay, 1951): $v = c - p + 2$, where v is the variance of the system, c is the number of components, and p is the number of phases. In our study, c = 3 (PS, Ca^{2+}, and H_2O can undergo independent concentration changes). The temperature and the pressure are specified in our studies to be 21 °C and 1 atm. When three phases coexist, the variance must be zero. Indeed, we observe that the composition of each phase is fixed. Hereafter we refer to the fixed value of the aqueous free Ca^{2+} concentration, when hydrated PS, $Ca(PS)_2$, and aqueous Ca^{2+} solution phases coexist, as "$[Ca^{2+}]^*$".[2]

The binding of Ca^{2+} between PS lamellae to form $Ca(PS)_2$ is described in terms of a dissociation constant, K_D, as in eq 3. By the convention that the thermodynamic activity of the pure condensed phases is unity, $K_D = \gamma[Ca^{2+}]^*$. However, the clearest physical picture of Ca^{2+} binding to PS is not in terms of K_D, but rather $[Ca^{2+}]^*$. At $[Ca^{2+}]$ below this critical value, the experiments can be described as showing "no binding of Ca^{2+} to PS" or "complete dissociation of $Ca(PS)_2$". At $[Ca^{2+}] > [Ca^{2+}]^*$, PS binds Ca^{2+} to form $Ca(PS)_2$.

These observations of the phase behavior of PS, Ca^{2+}, and water are organized in a pseudoternary phase diagram in Figure 4. This diagram also shows likely, but unexplored, regions in order to complete the description. The presence of components, namely Pipes buffer, KCl, and Ca^{2+} chelator, in addition to those at the apexes of the triangle, is neglected. This diagram is based upon observations (i–iv) and principles (v–ix): (i) a pure phase of $Ca(PS)_2$ can form; (ii) when $Ca(PS)_2$ and hydrated PS coexist, the aqueous Ca^{2+} concentration is fixed at $[Ca^{2+}]^*$; (iii) in excess $[Ca^{2+}]$ of 1, 10, and 100 mM, all PS is in the form $Ca(PS)_2$; (iv) for $[Ca^{2+}] < [Ca^{2+}]^*$, a hydrated PS phase and an aqueous phase coexist, with virtually all Ca^{2+} in the aqueous phase; (v) PS takes up water and exists as a single phase until water is in excess; (vi) addition of excess water to hydrated PS results in coexistence of an aqueous phase containing very little PS; (vii) the hydrated PS phase is expected to bind some Ca^{2+}, although the amount bound has been too small to measure. Nonetheless, the diagram indicates that a trace of Ca^{2+} can bind to hydrated PS; (viii) an aqueous phase can exist containing very low [PS], probably in a mi-

[2] This case is analogous to the classic example in the study of thermodynamics, $CaCO_3 \rightleftharpoons CaO + CO_2$. Here, c = 2. If temperature is a constant, then when three phases coexist, v = 0. The thermodynamic activity of CO_2 is given by the pressure of CO_2. $CaCO_3$ and CaO are each pure phases (solid solutions are not formed). The meaning of v = 0 is that at a given temperature the CO_2 pressure is fixed whenever the three phases coexist. If the pressure is made lower than this specified value at this temperature, the three phases will not be at equilibrium, and all $CaCO_3$ will change to $CaO + CO_2$ (Findlay, 1951, pp 10, 11, 212–215).

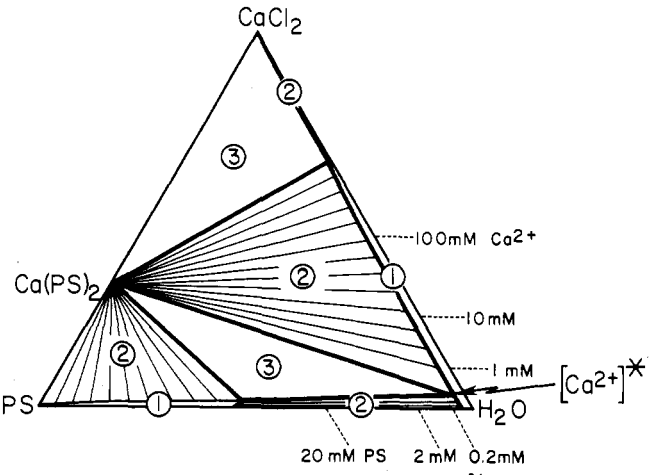

FIGURE 4: Pseudoternary phase diagram for Ca^{2+}, PS, and water. Pressure is constant at 1 atm, temperature at 21 °C. The presence of Pipes buffer, KCl, and Ca^{2+} chelator is neglected. The diagram is not drawn to scale. The number of coexisting phases is shown as a circled number in the center of a region. Regions of the diagram where data were obtained are heavily outlined. The range of PS concentrations studied, 0.2–20 mM, is shown on an axis ranging from pure PS to pure water. The range of Ca^{2+} concentrations studied, ~0.05 μM–100 mM, is shown on an axis ranging from pure $CaCl_2$ to pure water. The stoichiometry of the $Ca(PS)_2$ phase is correctly scaled on a mole fraction basis between pure PS and pure $CaCl_2$. The invariant Ca^{2+} concentration $[Ca^{2+}]^*$ is shown in coexistence with $Ca(PS)_2$ and hydrated PS. Tie lines are shown in the two-phase regions.

cellar state; (ix) $CaCl_2$ has limited solubility in water, precipitating as a hydrated solid at low water concentration.

Figure 4 is not drawn to scale. The range of PS concentrations studied, 0.2–20 mM, is shown on an axis ranging from pure PS to pure water. The range of Ca^+ concentrations studied, ~0.05 μM–100 mM, is shown on an axis ranging from pure $CaCl_2$ to pure water. Only the stoichiometry of the $Ca(PS)_2$ phase is correctly scaled on a mole fraction basis between pure PS and pure $CaCl_2$.

Finally, we note that the region of low-water and high-PS content is likely to have complex phase behavior, which is not indicated on the diagram.

Physical Adsorption. Ca^{2+} binding to PS was not detected for $[Ca^{2+}] < [Ca^{2+}]^*$. However, this is precisely the region (low θ) that would manifest the occupation of the highest affinity sites by a physical adsorption mechanism (de Boer, 1953). We conclude that physical adsorption is not significant at the low $[Ca^{2+}]$ examined here. Nonetheless, some Ca^{2+} is expected to bind (albeit a trace amount), and this is so indicated in Figure 4.

Veith and Sposito (1977) studied the somewhat analogous systems of OH^- binding to Fe- or Al-saturated ion-exchange resin and Cl^- binding to Ag-saturated ion-exchange resin. These investigators showed that a Langmuir adsorption analysis is untenable when precipitation of the binding ion occurs, i.e., phase separation. However, to detect the failure of an adsorption model correctly to describe the observed binding requires that measurements be made at very low adsorbent concentrations, i.e., before the onset of significant binding.

Variation of $[Ca^{2+}]^*$ with θ. For DOPS, $[Ca^{2+}]$ varies from ~2.7 μM at the start of binding to ~3.8 μM at $\theta = 0.7$ and thereafter increases markedly as θ approaches unity. For POPS, $[Ca^{2+}]$ varies from ~0.12 to ~0.17 μM over this range of θ. For BBPS, $[Ca^{2+}]$ is ~0.24 μM when binding starts and ~0.7 μM when $[Ca^{2+}]$ begins to increase rapidly. These observations apply to the entire range of initial PS concentrations examined and do not seem to be dependent on the amount of Ca^{2+} added or the amount of $Ca(PS)_2$ dissolved or the protocol of sample preparation. One interpretation of the observed small variation in $[Ca^{2+}]^*$ is that because the binding occurs far from equilibrium, the details of the properties of the $Ca(PS)_2$ lattice might depend upon the nature and number of lattice defects. These defects might be increased by prior formation of $Ca(PS)_2$ domains, as the later forming domains encounter the preexisting domains. When a large fraction of sites is occupied, perhaps near $\theta = 0.7$, formation of small domains with a large perimeter to area ratio and perhaps increased packing defects would be less favorable, requiring higher values of $[Ca^{2+}]$ for further binding.

A different interpretation of the small variation of $[Ca^{2+}]^*$ with θ is that the PS and/or $Ca(PS)_2$ are only approximately pure phases and to a small extent involve solid solution formation that is a variable over the course of the binding.

The much larger variation in $[Ca^{2+}]$ during binding of BBPS compared to POPS or DOPS is likely to have a different origin than discussed above. Whereas every molecule of DOPS has two C18:1 hydrocarbon chains, and every POPS has one C16:0 and one C18:1 chain, molecules of BBPS differ among each other in hydrocarbon chain composition. An analysis by Ohki et al. (1981) shows a BBPS sample to have 40 mol % C18:0, 31% C18:1, 6% C20:1, 6% C20:5, and smaller percentages of eight other fatty acyl chains. This mixture of chain types could result in a broader range of $[Ca^{2+}]$ during binding, if the different species have slightly different affinities for Ca^{2+}. This conjecture is reasonable considering the different affinities observed for DOPS compared to POPS.

Dependence of $[Ca^{2+}]$ on PS Type. There are significant differences in Ca^{2+} affinity among DOPS, POPS, and BBPS. Since only three PS types have been examined, generalizations are not strongly supported. At this point we note the following: (i) DOPS has the lowest lamellar gel–fluid transition temperature (−11 °C; Browning & Seelig, 1980) and has also the least affinity for Ca^{2+} ($[Ca^{2+}]^* = 3.0$ μM). In comparison, the POPS gel–fluid transition is at +13 to +14 °C (Martin Caffrey, unpublished experiments), with $[Ca^{2+}]^* = 0.14$ μM. The BBPS gel–fluid transition spans −1 to +15 °C (Boggs et al., 1977), with $[Ca^{2+}]^* \sim 0.25$–~0.7 μM. (ii) POPS and BBPS have similar acyl chains. They are also similar in the temperature of the gel–fluid transition and similar in the value of $[Ca^{2+}]^*$ during binding.

Comparison to Previous Studies. Several laboratories have measured Ca^{2+} binding to PS and found significant binding to begin in the range $[Ca^{2+}] \sim 0.1$–10 mM (Hendrickson & Fullington, 1965; Lansman & Haynes, 1975; Nir et al., 1978; Portis et al., 1979; Morris et al., 1979; McLaughlin et al., 1981; Ekerdt and Papahadjopoulos, 1981; Tilcock & Cullis, 1981; Silvius & Gagné, 1984). Only one laboratory has measured such high-affinity binding as is described herein. In a series of papers (Ohnishi and Ito, 1974; Tokutomi et al., 1981; Ohnishi & Tokutomi, 1981) this group reported that Ca^{2+}, at concentrations in the range 0.1–1 μM, binds to PS and mixtures of PS/PE and PS/PC. The experiments used ESR spectroscopy of labeled lipids to detect Ca^{2+} binding to PS multilayers supported in Millipore filters. It should now be appreciated that this sytem (i) holds the lipid in the multilamellar form and (ii) provides access of Ca^{2+} to sites between lamellae.

A clear demonstration that Ca^{2+} binding between PS lamellae is different in important ways from Ca^{2+} binding at the aqueous PS surface was reported by Portis et al. (1979). These investigators used X-ray diffraction to detect a short

lamellar repeat, suggesting Ca^{2+}-induced dehydration, and differential scanning calorimetry to find a greatly increased "melting" temperature for $Ca(PS)_2$ prepared from BBPS compared to hydrated BBPS, of 130 °C compared to 0–15 °C. In addition, several sharp lines in the wide-angle region of the diffraction pattern of $Ca(PS)_2$ are not present in the pattern of hydrated PS gel phase. These observations are all confirmed and extended for $Ca(PS)_2$ formed from a series of PS types (Hauser & Shipley, 1984).

Protocols To Provide Ca^{2+} Access between Lamellae. The penetration of a closed lipid bilayer is slow for most ions, including Ca^{2+}. Nonetheless, simply incubating hydrated PS with Ca^{2+}-containing buffer for 12–24 h results in Ca^{2+} binding, and many measurement shown in Figure 1 used this simple protocol. However, we did not know in advance of the results whether the details of conditions during Ca^{2+} binding would strongly affect the properties of the $Ca(PS)_2$ phase. Since no protocol-dependent differences were found in the final, equilibrium value of $[Ca^{2+}]^*$, we conclude that the properties of $Ca(PS)_2$ and PS that influence thermodynamic activity are virtually the same for every protocol.

Some protocols involve freezing in liquid N_2 and then thawing. We and others have previously used this procedure to equilibrate impermeant substances across bilayer vesicles (Feigenson, 1983; Oku & MacDonald, 1983; Tilcock et al., 1984). Since this protocol involves lowering the temperature below the gel–fluid phase transition temperature of the lipids, the possibility exists that the temperature-induced gel phase might bind Ca^{2+} differently than would the fluid lipid phase. To circumvent this possibility, the freezing process was performed at −10 °C, just warmer than the gel–fluid transition temperature of DOPS. The data shown in Figure 1 reveal that the details of the freezing are not important in this kind of experiment. Caution should remain, however, especially when lowering the temperature of a lipid mixture, if irreversible phase separation is possible.

Obtaining the same equilibrium value of $[Ca^{2+}]^*$ for every protocol strengthens the conclusion that a true thermodynamic characteristic of the PS–aqueous Ca^{2+} equilibrium has been found.

Use of Ca^{2+} Chelators. In preliminary experiments using EGTA to modulate $[Ca^{2+}]$, pH changes were found to be unacceptably large (e.g., 0.15 pH unit for formation of 3 mM Ca–EGTA as Ca^{2+} at initial pH 7.00 binds to EGTA at initial pH 7.00 in 100 mM Pipes–KCl buffer; resultant change in K_D for Ca–EGTA is 2-fold). This problem is well-known and can be minimized by titrating with base the H^+ released by EGTA (Campbell, 1983). However, it is far more convenient to use Ca^{2+} chelators that are fully ionized at pH 7. The chelators BrBAPTA and BAPTA, originally synthesized by Tsien (1980), have their highest pK_a's at 5.6 and 6.36, respectively. Furthermore, the Ca^{2+} affinities of these two chelators differ by 10-fold, making possible a choice of chelator K_D to approach more closely the $[Ca^{2+}]$ to be measured, thereby affording more accuracy. Finally, BrBAPTA and BAPTA are indicator dyes, with UV spectra sensitive to Ca^{2+} binding. Each dye has a convenient isosbestic point, so that corrections can be made for uncontrolled dye concentration changes (for example, from pipetting errors, transfer inefficiency, or solution evaporation). We note that the K_D values used here are calculated from Ca^{2+} and chelator *concentrations* but also from H^+ *activity* (pH), as in Grynkiewicz et al. (1985).

Supersaturation. The combination of two substances to form a third via a first-order phase transition commonly involves supersaturation, unless nuclei are present and accessible. For example, although the solubility product for $BaSO_4$ is 10^{-10} M^2, exceeding this solubility product by 25-fold did not give a $BaSO_4$ precipitate even after 1 month. To obtain immediate precipitation of $BaSO_4$ required exceeding the solubility product by $\sim 10^4$-fold (Von Weimarn, 1908). The barrier to the equilibrium is the formation of nuclei, which have a high free energy because of significant surface free energy and the high ratio of area to volume of small particles.

In the case of formation of $Ca(PS)_2$, different ways of adding Ca^{2+} to PS are observed to influence the supersaturation as shown in Figure 3. We can speculate that surface free energy would be different at the interface of dry or partially hydrated $PS/Ca(PS)_2$ compared to that of fully hydrated $PS/Ca(PS)_2$ and might be significantly different at the various temperatures involved in freeze–thawing compared to room temperature. Other speculations can be made based upon the possible protocol-dependent size of nuclei.

The least hypothetical aspect of supersaturation is that it is to be avoided for equilibrium measurements. Earlier workers solved this problem in studies of, for example, $BaSO_4$ and AgCl (Melcher, 1910) and other relatively insoluble substances by first preparing the substance (exceeding saturation) and then dissolving the substance under the ionic and thermal conditions of interest. We follow this idea by adding Ca^{2+} to PS and then partially dissolving the $Ca(PS)_2$ in EGTA, BrBAPTA, or BAPTA. In principle, no Ca^{2+} chelator is required, and a mixture of $Ca(PS)_2$ and PS could be washed with Ca^{2+}-free buffer and resuspended and the $[Ca^{2+}]$ measured. However, multivalent cation contamination makes this method unreliable for measuring $[Ca^{2+}]$ less than about 10 μM.

Significance. The values of $[Ca^{2+}]^*$ during formation of $Ca(PS)_2$, for the PS species examined, range from 3.0 μM for DOPS to 0.14 μM for POPS. These experiments use PS without other lipids. In a multicomponent membrane, we expect that the $[Ca^{2+}]$ required for $Ca(PS)_2$ phase separation would increase as the mole fraction of PS in the bilayer decreases. Even with this note of caution, the prediction of profound membrane rearrangements caused by a change in $[Ca^{2+}]$ from ~ 0.1 to ~ 10 μM is seen to be firmly based on simple physical chemistry. Because the formation of $Ca(PS)_2$ induces contact of two bilayers, the biological phenomenon of Ca^{2+}-dependent membrane fusion might involve, as one step in a multistep process, a phase transition of the sort described here.

ACKNOWLEDGMENTS

I am grateful for Martin Caffrey's assistance in performing preliminary experiments and providing unpublished data, and I thank him also for many helpful discussions. I also thank Sydney Ross, Mark Yeager, and Kathryn Florine for helpful discussions.

Registry No. DOPS, 70614-14-1; POPS, 40290-44-6; Ca, 7440-70-2.

REFERENCES

Bentz, J., Düzgünes, N., & Nir, S. (1983) *Biochemistry 22*, 3320–3330.

Boggs, J. M., Wood, D. D., Moscarello, M. A., & Papahadjopoulos, D. (1977) *Biochemistry 16*, 2325–2329.

Browning, J., & Seelig, J. (1980) *Biochemistry 19*, 1262–1270.

Budesinsky, B. (1969) in *Chelates in Analytical Chemistry* (Flaschka, H. D., & Barnard, A. J., Eds.) Vol. 2, pp 21–22, Marcel Dekker, New York.

Campbell, A. K. (1983) *Intracellular Calcium*, Wiley, Chichester.

Chen, P. S., Jr., Toribara, T. Y., & Warner, H. (1956) *Anal. Chem. 28*, 1756–1758.
de Boer, J. H. (1953) *The Dynamical Character of Absorption*, p 58, Clarendon, Oxford.
Eckerdt, R., Dahl, G., & Gratzl, M. (1981) *Biochim. Biophys. Acta 646*, 10–22.
Eckerdt, R., & Papahadjopoulos, D. (1982) *Proc. Natl. Acad. Sci. U.S.A. 79*, 2273–2277.
Feigenson, G. W. (1983) *Biochemistry 22*, 3106–3112.
Findlay, A., (1951) *The Phase Rule* (Campbell, A. N., & Smith, N. O., Eds.) 9th ed., pp 7–19, 277–281, Dover Publications, New York.
Gratzer, W. B., & Beaven, G. H. (1977) *Anal. Biochem. 81*, 118–129.
Grynkiewicz, G., Poenie, M., & Tsien, R. Y. (1985) *J. Biol. Chem. 260*, 3440–3450.
Hauser, H., & Shipley, G. G. (1984) *Biochemistry 23*, 34–41.
Hendrickson, H. S. & Fullington, J. G. (1965) *Biochemistry 4*, 1599–1605.
Hong, K., Düzgünes, N., Eckerdt, R., & Papahadjopoulos, D. (1982) *Proc. Natl. Acad. Sci. U.S.A. 79*, 4642–4644.
Kingsley, P. B., & Feigenson, G. W. (1979) *Chem. Phys. Lipids 24*, 135–147.
Lansman, J. & Haynes, D. H. (1975) *Biochim. Biophys. Acta 394*, 335–347.
Llinás, R., Steinberg, I. Z., & Walton, K. (1976) *Proc. Natl. Acad. Sci. U.S.A. 73*, 2918–2922.
McLaughlin, S., Mulrine, N., Gresalfi, G. V., & McLaughlin, A. (1981) *J. Gen. Physiol. 77*, 445–473.
Melcher, A. C. (1910) *J. Am. Chem. Soc. 32*, 50–66.
Morris, S. J., Chiu, V. K. C., & Haynes, D. H. (1979) *Membrane Biochem. 2*, 162–202.
Nir, S., Newton, C., & Papahadjopoulos, D. (1978) *Biochem. Bioenerg. 5*, 116–133.
Ohnishi, S.-I., & Ito, T. (1974) *Biochemistry 13*, 881–887.
Ohnishi, S.-I., & Tokutomi, S. (1981) in *Biological Magnetic Resonance* (Berliner, L., & Reuben, J., Eds.) Vol. 3, pp 121–153, Plenum, New York.
Oku, N., & MacDonald, R. C. (1983) *Biochemistry 22*, 855–863.
Portis, A., Newton, C., Pangborn, W., & Papahadjopoulos, D. (1979) *Biochemistry 18*, 780–790.
Silvius, J. R., & Gagnê, G. (1984) *Biochemistry 23*, 3232–3240.
Tilcock, C. P. S., & Cullis, P. R. (1981) *Biochim. Biophys. Acta 641*, 189–201.
Tilcock, C. P. S., Bally, M. B., Farren, S. B., Cullis, P. R., & Gruner, S. M. (1984) *Biochemistry 23*, 2696–2703.
Tokutomi, S., Lew, R., & Ohnishi, S.-I. (1981) *Biochim. Biophys. Acta 643*, 276–282.
Tsien, R. Y. (1980) *Biochemistry 19*, 2396–2404.
Veith, J. A., & Sposito, G. (1977) *Soil Sci. Soc. Am. J. 41*, 697–702.
Von Weimarn, P. P. (1908) *Koll. Z. 3*, 282–304.

Specific Substitution into the Anticodon Loop of Yeast Tyrosine Transfer RNA†

Lance A. Bare and Olke C. Uhlenbeck*
Department of Chemistry and Biochemistry, University of Colorado, Boulder, Colorado 80309
Received January 23, 1986; Revised Manuscript Received May 15, 1986

ABSTRACT: The aminoacylation kinetics of 19 different variants of yeast $tRNA^{Tyr}$ with nucleotide substitutions in positions 33–35 were determined. Substitution of the conserved uridine-33 does not alter the rate of aminoacylation. However, substitution of the anticodon position 34 or position 35 reduces K_m from 2- to 10-fold and V_{max} as much as 2-fold, depending on the nucleotide inserted. The ochre and amber suppressor $tRNAs^{Tyr}$ both showed about a 7-fold reduction in V_{max}/K_m. Data from $tRNA^{Tyr}$ with different modified nucleotides at position 35 suggest that specific hydrogen bonds form between the synthetase and both the N1 and N3 hydrogens of Ψ-35. The effect of simultaneous substitutions at positions 34 and 35 can be predicted reasonably well by combining the effects of single substitutions. These data suggest that yeast tyrosyl-tRNA synthetase interacts with positions 34 and 35 of the anticodon of $tRNA^{Tyr}$ and opens the possibility that nonsense suppressor efficiency may be mediated by the level of aminoacylation.

The anticodon loop of many tRNAs[1] form part of the recognition site for their cognate aminoacyl-tRNA synthetase (Kisselev, 1985). In the case of the yeast tyrosine tRNA, the available data appear contradictory. On one hand, two suppressor tRNAs derived from the $tRNA^{Tyr}$ by single-base substitutions of the wobble anticodon nucleotide G-35 still insert tyrosine into protein, suggesting that the substitution does not interfere with their ability to aminoacylate (Piper et al., 1976; Goodman et al., 1976). In addition, removal of the anticodon nucleotides 34–36 from the closely related *Torula utilis* $tRNA^{Tyr}$ does not eliminate aminoacylation by yeast tyrosoyl-tRNA synthetase (Hashimoto et al., 1972). On the other hand, the yeast $tRNA^{Tyr}$ precursor containing a 15-nucleotide intron in the anticodon loop does not aminoacylate (Valenzuela et al., 1980), despite the fact that the structure of the remainder of the tRNA appears to be normal (Swerdlow & Guthrie, 1984). Furthermore, in a previous paper, we

† This work was supported by a grant from the National Institutes of Health (GM 30418).

[1] Abbreviations: $tRNA^{Tyr}$, yeast tyrosine transfer RNA; pNp, nucleoside 3′,5′-bisphosphate; Hepes, *N*-(2-hydroxyethyl)piperazine-*N*′-2-ethanesulfonic acid; Tris, 2-amino-(2-hydroxylmethyl)-1,3-propanediol; TCA, trichloroacetic acid; DTT, dithiothreitol; BSA, bovine serum albumin.

0006-2960/86/0425-5825$01.50/0